Medical Engineering and Physics 000 (2016) 1–10

Contents lists available at ScienceDirect

Medical Engineering and Physics

journal homepage: www.elsevier.com/locate/medengphy

EEG-based BCI for the linear control of an upper-limb neuroprosthesis

Carmen Vidaurre[a,*], Christian Klauer[b], Thomas Schauer[b], Ander Ramos-Murguialday[c,d], Klaus-Robert Müller[a,e,f,*]

[a] Machine Learning Group, Computer Science Faculty, Berlin Institute of Technology, Berlin, Germany
[b] Control Systems Group, Berlin Institute of Technology, Berlin, Germany
[c] Institute for Medical Psychology and Behavioral Neurobiology (IMP), University of Tübingen, Tübingen 72076, Germany
[d] TECNALIA, San Sebastian, Spain
[e] Bernstein Focus: Neurotechnology, Berlin, Germany
[f] Department of Brain and Cognitive Engineering, Korea University, Anam-dong, Seongbuk-gu, Seoul 136-713, Republic of Korea

ARTICLE INFO

Article history:
Received 8 January 2016
Revised 18 April 2016
Accepted 7 June 2016
Available online xxx

Keywords:
Brain–computer interfacing
Motor imagery
Neuralprosthesis
Functional electrical stimulation

ABSTRACT

Assistive technologies help patients to reacquire interacting capabilities with the environment and improve their quality of life. In this manuscript we present a feasibility study in which healthy users were able to use a non-invasive Motor Imagery (MI)-based brain computer interface (BCI) to achieve linear control of an upper-limb functional electrical stimulation (FES) controlled neuro-prosthesis. The linear control allowed the real-time computation of a continuous control signal that was used by the FES system to physically set the stimulation parameters to control the upper-limb position. Even if the nature of the task makes the operation very challenging, the participants achieved a mean selection accuracy of 82.5% in a target selection experiment. An analysis of limb kinematics as well as the positioning precision was performed, showing the viability of using a BCI–FES system to control upper-limb reaching movements. The results of this study constitute an accurate use of an online non-invasive BCI to operate a FES-neuroprosthesis setting a step toward the recovery of the control of an impaired limb with the sole use of brain activity.

1. Introduction

A main concern for patients who suffered a stroke, a traumatic brain injury or a spinal cord injury is the difficulty to normally perform daily life activities. Many assistive technologies have been developed in order to increase their independence and help them reacquire interacting capabilities with the environment. In particular, neuro-prostheses are very promising tools to achieve this goal [1]. They are electronic devices that can be used to operate a mechanical orthosis (cf. [2]), or to control paralyzed muscles as reported elsewhere [3–5]. Functional electrical stimulation (FES) is commonly used to recover functionality in paralyzed or dysfunctional limbs and is also used together with neuroprostheses to develop advanced systems. FES-neuroprostheses can be operated with a manual switch, movements of a non-damaged muscle or by residual muscle activity (electromyography) to support the user's movement attempt (cf. [5,6]). When the state of the disease prevents the use of all of the aforementioned operational approaches, brain computer interfaces (BCI) are emerging as an alternative. BCIs are systems that aim to provide control over a computer application or a device by inferring the user's intention from the ongoing brain signal [7,8]. In this manuscript we describe the use of a FES-driven neuroprosthesis using a non-invasive BCI system operating with electroencephalographic signals (EEG), where EEG is processed to control the FES-neuroprosthesis. There have been previous attempts to couple EEG-based BCIs and neuro-prostheses. Event-related potentials (ERP) and steady state visually evoked potential (SSVEP) measured with EEG have been used as stimuli to control neuroprostheses [9–11]. In this manuscript we report the use of another type of signal measured when the participant performs the imagination of movements of the limbs (motor imagery, MI). Neuroprostheses driven by MI have been reported in [6] and [12]. These works propose the use of a BCI as a brain-switch, in order to achieve a sequential operation for the restoration of hand grasp function in a tetraplegic patient in [6], or to turn on/off the stimulation to trigger hand (and thumb) opening and closing in healthy users in [12].

In this study, we present a more sophisticated task: namely we show that it is possible to move an arm toward one of several objects with the help of FES. The position of the arm is

* Corresponding author. Fax: +49 3031478622.
E-mail addresses: carmen.vidaurre@tu-berlin.de (C. Vidaurre), klaus-robert.mueller@tu-berlin.de (K.-R. Müller).

http://dx.doi.org/10.1016/j.medengphy.2016.06.010
1350-4533/

determined by the linear continuous control of a trial-based MI-BCI. Linear control is the real-time computation of the position of the arm by the translation of the BCI classification output into spatial coordinates. The real-time nature of the task makes the operation more challenging and demanding for the user than that of previous approaches [13], but also offers a more natural way to accomplish it.

However, to achieve effective linear BCI control, two imagery classes must be distinguished with a reliability of at least 80% of accuracy in single trial. Our previous work showed that above this threshold the output of the classifier can be used to determine in real-time the position on a given trajectory, [13]). Depending on the accuracy of the classifier, the user can gain good control of the exact stopping point of a movement along a trajectory. However, this was shown in a pure BCI system that did not include the stimulation of the arm by FES. In this manuscript we describe a feasibility study with seven healthy BCI users. All of them were able to gain control over the BCI–FES system and could select between 2 and 4 virtual targets from a table. The potential use of such a system in clinical applications is also discussed.

2. Methods

The experimental protocols were approved by the ethics committee of the University of Tübingen, Medical Faculty. All participants gave written consent and the study was performed in accordance with the Declaration of Helsinki.

2.1. Description of the brain computer interface

The parameters needed to calculate a classifier to discriminate MI activity are frequency band of interest, time interval where the class discrimination is maximized and spatial filters. These parameters are subject-specific and an optimizing procedure was used in order to determine them. Particularly, we used the methods described in [14–16].

After filtering and epoching the EEG in the optimal frequency band and time interval, the resulting signal was spatially filtered using Common Spatial Patterns (CSP). CSP is a technique used to analyze high dimensional data based on recordings from two brain activities leading to two different classes, e.g., imagining the movement of the left or the right hand. This spatial filtering method is widely used in BCIs based on Event Related De/Synchronization (ERD/S) [16]. The EEG signal is commonly band-pass filtered in a subject-selected frequency band in between 7 and 30 Hz. Two covariance matrices $\boldsymbol{\Sigma}_{\boldsymbol{EEG+}}$ and $\boldsymbol{\Sigma}_{\boldsymbol{EEG-}}$ are calculated for the two classes. CSP finds a spatial filter $\boldsymbol{w}_{\boldsymbol{CSP}}$ that maximizes the difference in the average band power of the filtered signal while keeping the sum constant. The problem can be solved as a generalized eigen-value problem:

$$\begin{aligned} &\underset{\boldsymbol{w}_{CSP}}{\text{argmax}} && \boldsymbol{w}_{\boldsymbol{CSP}}^{T}(\boldsymbol{\Sigma}_{\boldsymbol{EEG+}})\boldsymbol{w}_{\boldsymbol{CSP}} \\ &\text{subject to} && \boldsymbol{w}_{\boldsymbol{CSP}}^{T}(\boldsymbol{\Sigma}_{\boldsymbol{EEG+}}+\boldsymbol{\Sigma}_{\boldsymbol{EEG-}})\boldsymbol{w}_{\boldsymbol{CSP}}=1 \end{aligned} \tag{1}$$

Then, only a few filters are chosen using a heuristic approach as in [14]. Thus, the dimensionality of the features is reduced. After projecting the EEG into the selected filters, the natural logarithm is applied to normalize the signals and classify them using a Linear Discriminant Classifier (LDA), which has been shown to be an efficient classifier for motor imagery BCI data (see [15,17]). The signals collected in the calibration phase (without feedback) are used to train the LDA classifier. For two equally distributed classes, LDA is computed as follows:

$$o = \boldsymbol{w}_{\boldsymbol{LDA}}^{\top}\cdot\boldsymbol{x}+b \tag{2}$$

$$\boldsymbol{w}_{\boldsymbol{LDA}} = \boldsymbol{\Sigma}^{-1}\cdot(\boldsymbol{\mu}_{+}-\boldsymbol{\mu}_{-}) \tag{3}$$

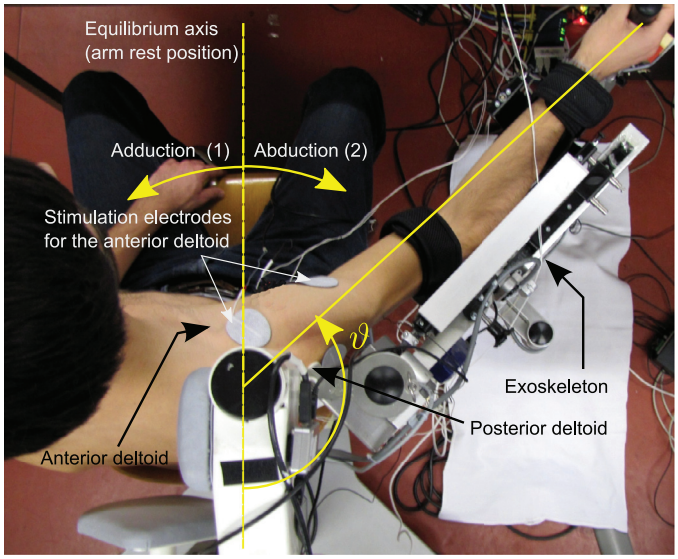

Fig. 1. Top view of the experimental set-up showing the exoskeleton, the stimulation electrodes and the angle definition.

$$\boldsymbol{\Sigma} = \boldsymbol{\Sigma}_{+}+\boldsymbol{\Sigma}_{-} \tag{4}$$

$$b = -0.5\cdot(\boldsymbol{\mu}_{+}+\boldsymbol{\mu}_{-})^{\top}\cdot\boldsymbol{w}_{\boldsymbol{LDA}} \tag{5}$$

where the output o is the distance of the feature vector $\boldsymbol{x}$ to the decision hyperplane perpendicular to the weight vector $\boldsymbol{w}_{\boldsymbol{LDA}}$. The location of the plane is defined by the bias b. If the o is negative, the class is - , otherwise, the class is + . $\boldsymbol{\Sigma}_{+}$ and $\boldsymbol{\Sigma}_{-}$ are the covariance matrices of the features of each class. Finally $\boldsymbol{\mu}_{-}$ and $\boldsymbol{\mu}_{+}$ are the mean values of the features of each class.

2.2. FES

Fig. 1 shows the FES set-up used in the experiments. The electrical stimulation of an antagonistic muscle pair at the shoulder consisting of the anterior and posterior deltoid enabled the horizontal shoulder abduction as well as the adduction of the arm, respectively. A passive exoskeleton (Armeo, Hocoma, see [18]) provided a weight compensation and additionally allowed the measuring of the horizontal joint angle ϑ. The elbow-joint and the shoulder abduction angles were not controlled by FES. Further, the humeral shoulder rotation was locked by the exoskeleton.

A stimulation system RehaStim (HASOMED GmbH, Magdeburg, Germany) was used to generate the electrical pulses applied to the muscles through self-adhesive hydro-gel electrodes at a frequency of $f_a = 25$ Hz.

For the anterior ($i = 1$) and the posterior ($i = 2$) deltoid, the current amplitudes $I_i \in [0, 90\text{mA}]$ and the pulse widths $pw_i \in [0,\ 500\mu\text{s}]$ for the bi-phasic stimulation pulses were obtained from the normalized pulse-charges v_i by means of the charge-control method as described in [19].

Based on the horizontal shoulder rotation angle measurement ϑ, a Proportional Derivative (PD)-feedback controller [20] adjusted the stimulation intensities for both muscles in order to rapidly follow a given reference sent by the BCI module.

Because two antagonistic muscles acting into opposite directions were actuated, the following switching strategy distributing a one-dimensional control (actuation) signal u to two stimulation intensities v_1 and v_2 was used:

$$\begin{pmatrix} v_1 \\ v_2 \end{pmatrix} = \begin{pmatrix} max(0, w\cdot u(t)) + v_{1,min} \\ max(0, -(1-w)\cdot u(t)) + v_{2,min} \end{pmatrix} \tag{6}$$

Please cite this article as: C. Vidaurre et al., EEG-based BCI for the linear control of an upper-limb neuroprosthesis, Medical Engineering and Physics (2016), http://dx.doi.org/10.1016/j.medengphy.2016.06.010

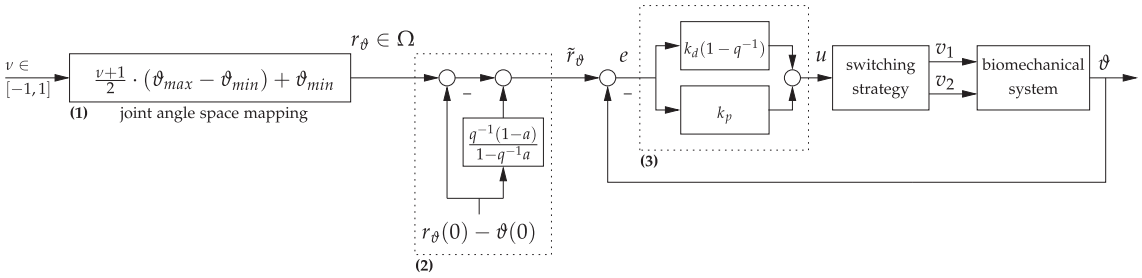

Fig. 2. The applied feedback control system including a target angle transformation **(1)**, the initial transient controlling circuit **(2)** and a PD-controller **(3)** are shown.

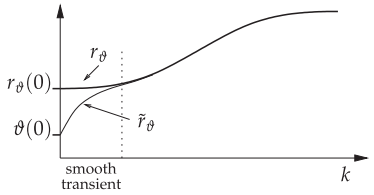

Fig. 3. Visualization of the effects caused by the transient control circuit: For initial derivations between target and actual joint-angle, a new reference $\tilde{r}_\vartheta$ is calculated that smoothly converges to target trajectory r_ϑ.

where $v_{i,min}$ was additionally applied in order to compensate for thresholds appearing in the recruitment curves (see [21]). The balancing factor $w \in [-1, 1]$, helped to produce a symmetric stimulation in both muscles. On top of the switching strategy, a discrete-time feedback controller as shown in Fig. 2 was applied to control the joint angle ϑ using the virtual actuation variable u. Here, q^{-1} is the one-step backward shift operator ($l(k)q^{-1} = l(k-1)$).

In a first step, the normalized angular position $\nu \in [-1, 1]$ provided by the BCI was linearly mapped by **(1)** into a joint angle space $\Omega := [\vartheta_{min}, \vartheta_{max}]$ that describes the reachable range achieved by FES. This range can be also seen as a predefined linear trajectory. The mapped angle was used as the target joint angle r_ϑ.

The normalized target position trajectory $\nu(0)$ started at zero, which corresponds to a joint angle reference r_ϑ in the center of the available space Ω. Typically, the initial joint angle $\vartheta(0)$ does not match the initial reference $r_\vartheta(0)$. This may introduce an unacceptable large initialization error in the control system, which could react with a sudden and large control actuation. In order to overcome this problem, a corrected reference $\tilde{r}_\vartheta$ was introduced and calculated by a transient controlling dynamical system **(2)**. The new reference angle trajectory started at the initial joint angle $\vartheta(0)$ and converged to r_ϑ, as illustrated in Fig. 3. The rate of convergence can be influenced by the parameter $a \in [0, 1]$. For all subjects $a = 0.98$ was a feasible choice. This value corresponds to a time interval of 4 s for reaching a convergence of approximately 90%.

Finally, a PD-controller **(3)** performed a reference trajectory tracking for the joint angle. An additional integral component in the controller could compensate for steady state errors. However, there is the drawback of potential instabilities and reduced robustness [22] and, therefore, an integrating part was intentionally omitted. The parameters for the proportional gain k_p and the derivative gain k_d were tuned during the activated control system as outlined in Section 2.4.2.

2.3. BCI–FES integration

Fig. 4 shows the architecture of the BCI–FES system. The BCI module was developed using the Berlin BCI proprietary software[1] ([23]) and deployed in a machine running Windows XP.

The FES-control system was installed in a separate PC running Linux with RT-Preemption-Patch. It was divided into a communication interface and the real-time control module. The former received the reference position and the commands for activation/deactivation of the controller via an UDP/XML-protocol and the latter included the hardware interfaces and the control algorithm described in Section 2.4.2. The implementation of the feedback controller activated by the state machine was done using OpenRTDynamics.[2] Commands for control activation along with a reference position were sent via UDP/XML from the BCI-module and interpreted in real-time in the FES-module.

2.4. Experimental procedure

2.4.1. BCI calibration

Data were recorded in one session from seven healthy BCI-users with previous experience (five had participated in one session and two in more than one). The brain activity was acquired from the scalp with multi-channel EEG amplifiers using 37 Ag/AgCl electrodes in an extended 10–20 system sampled at 1000 Hz with a band-pass filter from 0.05 to 200 Hz.

First, the users performed MI of three limbs (left hand, right hand and feet) within a calibration session (i.e., without feedback). Approximately every 8 s one of three different visual cues (arrows pointing left, right, or down) indicated to the participant the type of motor imagery task to perform. A 15 s break followed after every 20 trials. One run consisted of 60 trials (20 trials/class) and a total of three MI runs were recorded, resulting in 180 trials. Then, the calibration data was analyzed, a subject-selected frequency band and spatial filters were computed and only the pair of classes with best discriminability (left hand vs. foot or foot vs. right hand) was selected to later perform the feedback task. All users achieved a predicted performance of at least 80% of accuracy in this class pair. Then, the upper-limb not involved in the MI task was selected to deploy the neuro-prosthesis. Previous analyses with a similar setup showed that users were disturbed by the performance of MI and the stimulation in the same limb [24]. This selection assured that users could perform the task with sufficient accuracy.

2.4.2. FES calibration

At first, the maximal tolerable stimulation intensities $v_{i,max}$ and the joint angles ϑ_{min} and ϑ_{max} for the boundaries of the FES-reachable space Ω were obtained. In a following phase, the stimulation intensities v_i until the onset of muscular contraction were observed. The corresponding intensities represented the muscular thresholds $v_{1,min}$ and $v_{2,min}$ respectively. Initially, the balancing factor w from Eq. (6) was set to $w = 0.5$. A rectangular periodic test signal with the period N_p and Amplitude A was used to simulate u. The amplitude A was chosen to significantly excite the system such

[1] An open source version can be downloaded from http://bbci.de/toolbox.

[2] http://openrtdynamics.sf.net.

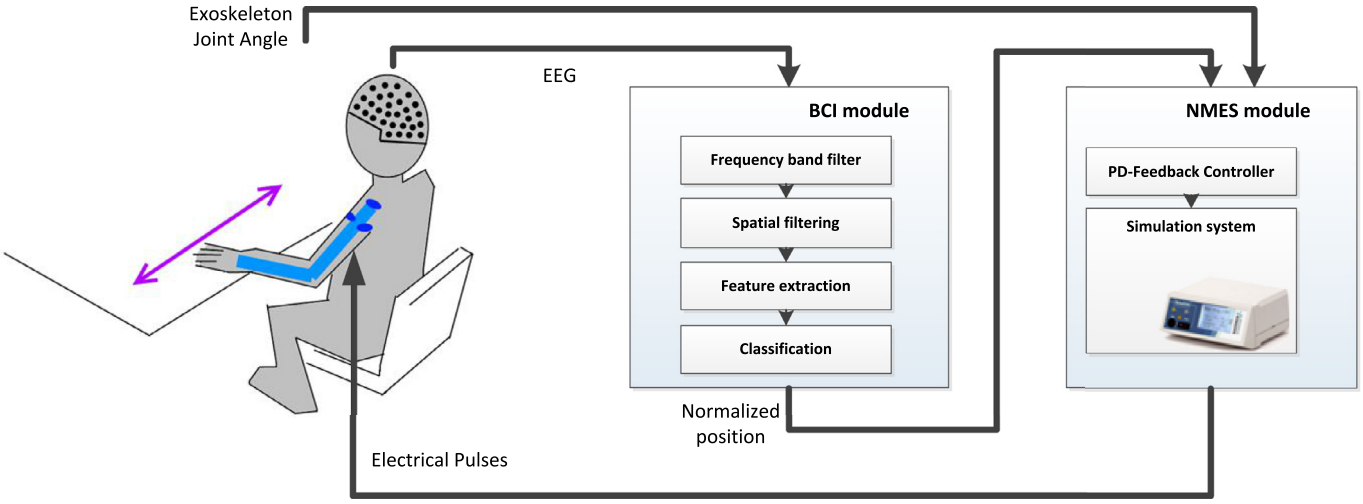

Fig. 4. Overview of the BCI–FES integration.

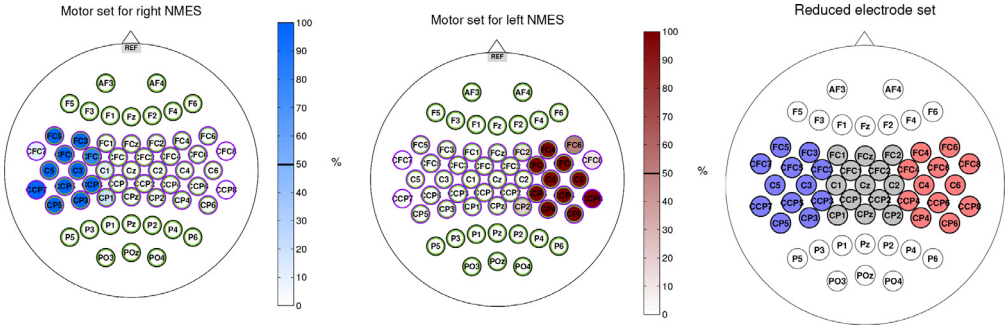

Fig. 5. Left: the dark-blue electrodes were selected by the algorithm as significantly noisy when the FES was recorded on the right arm. Middle: the dark-red electrodes were identified as significantly noisy when FES was recorded in the left arm. Right: electrodes used in the experimental setup. When the right arm was stimulated for the neuro-prosthesis, the sets in gray and red were chosen. Otherwise, the gray and blue were used. (For interpretation of the references to colour in this figure legend, the reader is referred to the web version of this article.)

that an angular movement of approximately 50% of the reachable space Ω was observed. The period N_p was chosen such that the response of the joint angle resulted in a clearly visible steady state at the end of each step. During the test, the factor w was tuned, such that the step responses into both directions were as symmetric as possible. Finally, the PD-controller parameters were empirically tuned in the activated loop. Therefore, the following trial and error procedure was performed: In a first step, the proportional gain k_p was increased until step-responses with the onset of an overshoot (when the joint angles shortly go beyond the target angles) were obtained, while setting $k_d = 0$. Then, the derivative gain k_d was increased until a step-response overshoot of 30% was achieved.

2.4.3. Removing the afferent FES activity from the EEG

FES and passive movement induce neural activation in the sensorimotor cortex. This occurs in the same frequency and time as the one induced by the imagination of the movement (see [24–26]). In this situation, the afferent activity interferes in the discrimination of the efferent one. If this disturbance is not reduced, it may cause a drop of the control accuracy of the system (cf. [13]). With this goal in mind, we developed a subject-independent algorithm (without the need of optimization for new users) to identify the electrodes that are most affected by the neural activity induced by FES and be able to remove them from the optimization of BCI features and classifier. The algorithm was optimized using recorded data from a group of ten participants, not coincident with those of the experiment presented in this manuscript. The algorithm was finally tested in online experiments, with another group of 10 participants. First, this procedure performed the filtering and segmentation of the EEG signal in a subject-optimized frequency band and time interval using motor imagery EEG and FES data of each individual. After computing the logarithm of the variance on each of the 37 electrodes depicted in the right panel of Fig. 5, the difference in band power between MI and FES in a specific channel was quantified and evaluated whether it was significant. For this purpose, electrode-wise paired z-tests of the differences of the two conditions were performed. These conditions were the MI of the two selected limbs and FES of the third limb. Although we did not compare MI of a limb against MI of the same limb with simultaneous FES, we showed in a previous work that in average NMES induces a significantly larger ERD/S effect in comparison to MI (for details see [24]). The z-scores are obtained calculating:

$$z = \frac{\bar{d} - \mu}{SE_{mean}} \tag{7}$$

where $\bar{d}$ is the sample mean of the differences and SE_{mean} the standard error of the mean. We assume the null hypothesis value 0 for the population mean μ, which implies that there are no differences between the two conditions, MI and NMES. The electrodes with z-score values outside the 95% percentile of the distribution ($z > 1.96$) can be selected as the ones most strongly affected by NMES (the band power differences are significant). We performed a leave one subject out cross-validation where the epochs of all

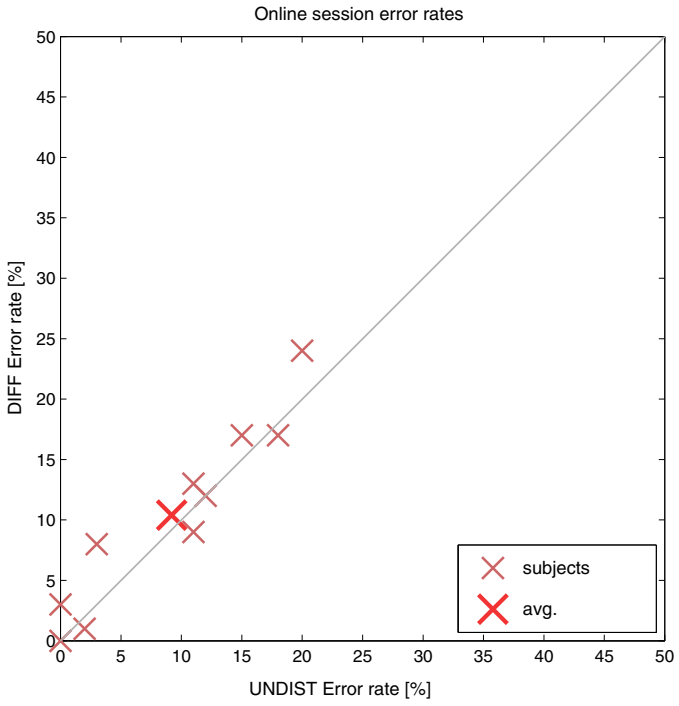

Fig. 6. Scatter plot comparing the on-line performance of 10 users with FES stimulation and without it (undisturbed MI).

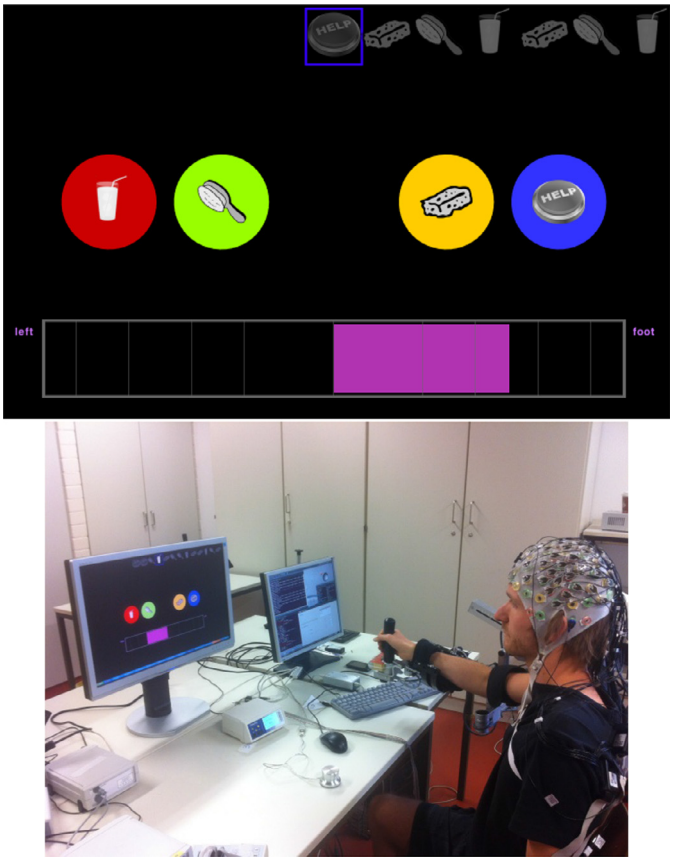

Fig. 7. Screen-shot of the BCI-feedback (up) and picture of the BCI-FES system experimental setup (down).

participants but one were used to compute the z-scores. The test error was then calculated using the test data of the remaining user. The resulting electrode sets can be seen in Fig. 5. The result of the analysis in pre-recorded data showed that the error using the 37 electrodes of the right panel in Fig. 5 is 17.95 ± 4.23 and by removing electrodes as aforementioned, the error is reduced to 16.02 ± 3.69. Additionally, the results of the previous off-line analysis were validated during on-line experiments. Data were acquired in a 1-day session from 10 healthy subjects using the same experimental environment as in the off-line session. The participants performed four runs with 50 trials each, which could be of two types, MI or MI+FES. The runs were conducted in pseudo-random order. The results are depicted in Fig. 6. When no stimulation was applied, the average error rate was 9.20 ± 2.36 using the complete electrode set. When stimulating the limb not involved in the MI-task and using only the 25 electrodes according to the pair of tasks selected, the error rate was 10.40 ± 2.45. A two-tailed paired Wilcoxon test revealed no significant differences between both conditions (p=0.14). This shows that the reduced electrode set allows users to perform BCI experiments without experiencing a performance drop. Given this, the technique was applied in the experiments presented in this manuscript.

2.4.4. Classifier adaptation

As introduced above, the MI signals were contaminated with afferent FES noise and a divergence between the undisturbed MI condition and the one containing FES was expected [24]. In this case, the classifier needs to be adjusted. A way to achieve this is to employ some type of adaptation [27,28]. In this system, class labels were not available during the online operation, therefore the classifier trained with MI data was re-adjusted using the unsupervised method *PMean* described in [29]. This method adapts the classifier in an unsupervised fashion after each trial by updating the pooled mean of the features (Eq. (5)). Although it is typically used to overcome the shift between the distributions of calibration and feedback data, it can also be used to adapt the MI trained LDA classifier to the test data containing MI and afferent activity (see [24]).

2.4.5. Feedback

Proprioceptive and visual feedback were delivered to the user. Proprioceptive feedback was achieved by the stimulation and the position of the arm. Visual BCI-feedback was given via a screen in front of the participant (see Fig. 7), and consisted of the control by means of MI of the movement of a bar. The speed at which the bar moved was determined by the magnitude of the classification output. The task of the participant was to use motor imagery to make the bar move into the target position indicated by the application. The control of the bar was relative to the actual position, i.e., at each update step a fraction of the classifier output was added to the actual cursor position: for every time update, the new length of the bar was the old length, shifted by an amount proportional to the classifier output.

An object list in the upper row of the monitor indicated which object had to selected in each trial. During the trial, the normalized position of the bar was sent to the FES subsystem in real-time. At the beginning of each trial, the cursor was set to the central position and was kept fixed for 750 to 1000 ms before it could start moving. Four (or two) symbols were distributed horizontally in the center of the screen representing objects in the table in front of the user. Under each symbol, two thresholds delimited the selection zone for that object. In order to select a symbol, the user had to maintain the bar between the corresponding thresholds. In order to facilitate stopping the bar movement between two thresholds, the progression of the bar was slowed down using a friction factor. No physical objects were placed on the table to avoid the

Table 1
Grand average performance, selection and confirmation time. The second column of the table corresponds to the selected pair of classes, the third one to the number of objects to be selected. The fourth column is the cross-validation error estimated in the parameter selection using the data of the calibration recording. The fifth, sixth and seventh columns are the percentages of hits, misses and rejects achieved in the feedback phase, respectively. Finally, the last column is the average length of the trial.

Subject	Classes	N	Calib. error	Hit (%)	Miss (%)	Reject (%)	Time (s)
A	Left-foot	4	0.0 ± 0.0	89.47	2.63	7.89	15.29
B	Left-foot	2	15.0 ± 11.7	71.05	27.63	1.32	22.15
C	Left-foot	4	5.0 ± 7.6	76.07	6.84	17.09	14.51
D	Left-foot	4	0.0 ± 0.0	92.37	0.00	7.63	12.08
E	Foot-right	2	1.7 ± 3.1	90.79	9.21	0.00	16.83
F	Foot-right	2	10.8 ± 11.8	80.52	18.18	1.30	16.81
G	Left-foot	4	5.0 ± 7.8	77.19	4.39	18.42	15.43
Mean ± SE				82.5 ± 3.2	9.8 ± 3.7	7.7 ± 2.9	16.2 ± 1.2

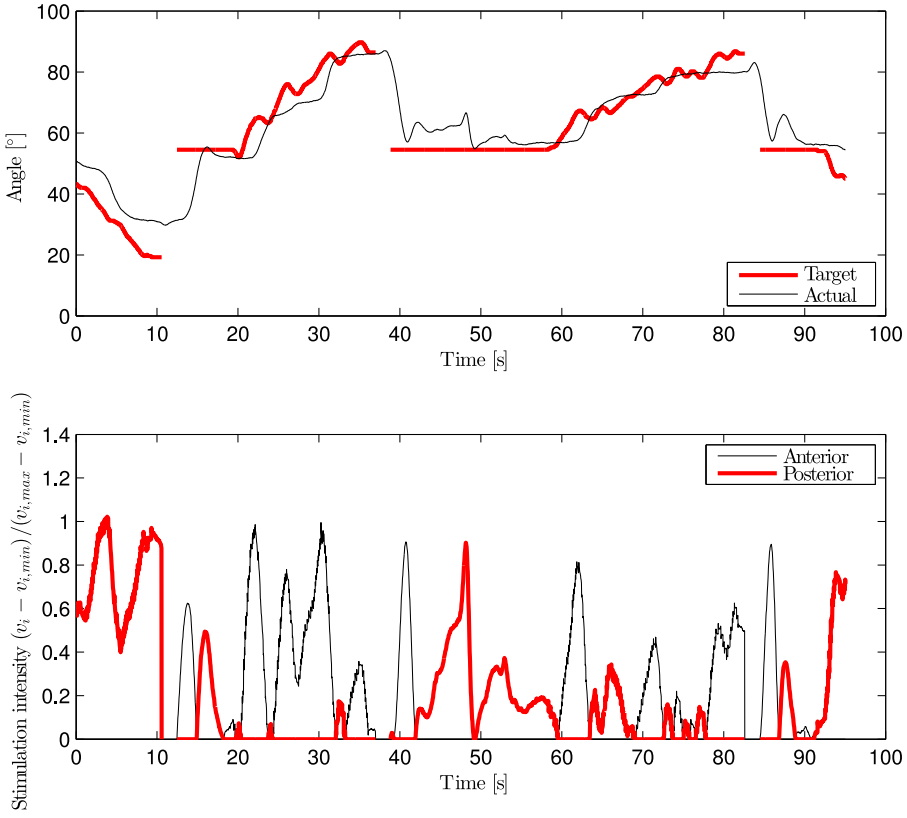

Fig. 8. Exemplary data of an FES-controlled arm movement for two sequences. The upper plot shows the target (thick line) along the actual angle (thin line) and the lower visualizes the required normalized stimulation intensities. For time instants during which the target angle is not shown, the experiment was paused for 2 s. (For interpretation of the references to colour in the text, the reader is referred to the web version of this article.)

unconscious modification of the arm position by the users during the object selection.

After the sensible parameters were computed (frequency band, time interval, CSP filters and classifier) and before the on-line recording, a short feedback run without stimulation was performed in order to empirically select the growing speed of the bar and the selection time. During this test, the users also tried different strategies to stop the motion between thresholds. Usually a short (1–2 s) imagination of the other limb was chosen. This post-calibration procedure allowed to evaluate the ability of the user to stop the bar between the thresholds of four objects. If this goal was not easily achievable, the feedback recording was performed with only two objects. Then, participants performed two or three runs of 40 trials each. The trial was considered successful if the user could maintain the bar between the thresholds for a predefined time (ranging from 2.5 to 4 s depending on the user).

3. Results

3.1. BCI

Accuracy (% of successfully completed trials) and time required to select an object were used as performance measures for the BCI-module. The average accuracy achieved by the participants was 82.50 ± 3.16. This value is well above the minimum control accuracy of 70% described by [30] for two-class BCI systems. Table 1 summarizes the results for each participant, where the second column corresponds to the selected tasks and the third one to the number of objects that the users was able to select. The fourth column is the cross-validation error estimated in during the parameter selection using the data of the calibration recording. The fifth, sixth and seventh columns are the percentages of hits, misses and rejects achieved in the feedback phase, respectively. Finally, the last column is the average length of the trial.

Please cite this article as: C. Vidaurre et al., EEG-based BCI for the linear control of an upper-limb neuroprosthesis, Medical Engineering and Physics (2016), http://dx.doi.org/10.1016/j.medengphy.2016.06.010

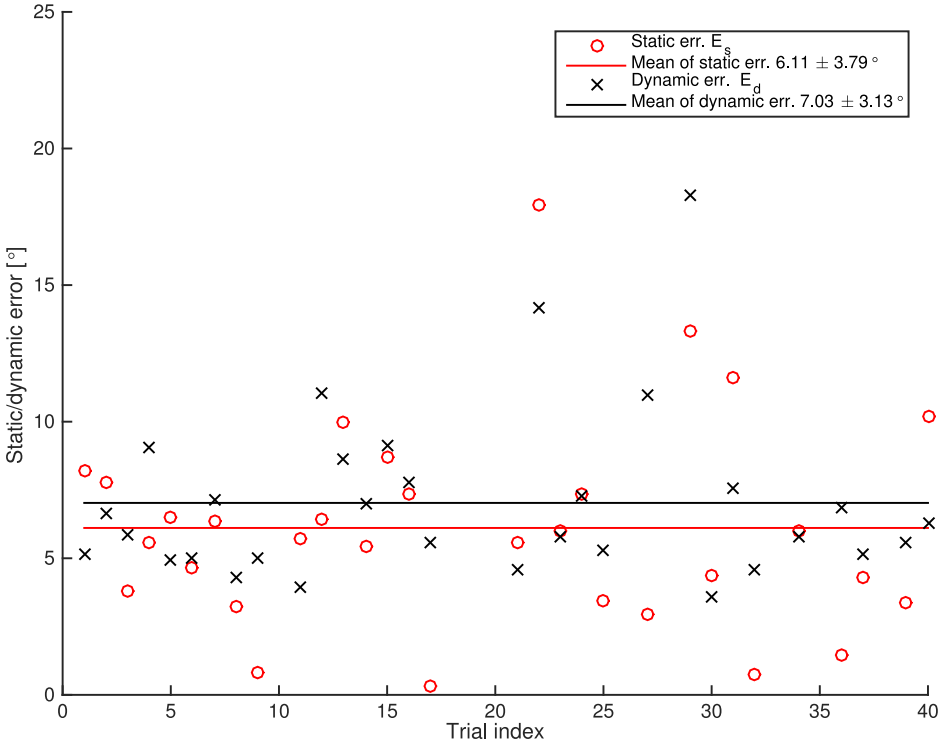

Fig. 9. Exemplary error analysis for one subject and 40 trials. The steady state error by the end of the selection and the dynamic error considering the whole trial are shown.

Table 2
Grand average movement range, mean values and standard deviations of steady state E_S and dynamic error E_D. The values in brackets describe the relative error with respect to the movement range.

Subject	Movement range (°)	E_S (°)	E_D (°) (RMS)
A	71.96	6.44 ± 5.65 (8.9%)	8.83 ± 4.46 (8.95%)
B	62.03	13.84 ± 9.95 (22.3%)	12.72 ± 6.98 (22.3%)
C	32.46	7.58 ± 3.91 (23.3%)	8.25 ± 4.6 (23.4%)
D	64.46	7.45 ± 3.91 (11.5%)	8.78 ± 3.12 (11.5%)
E	83.76	17.50 ± 13.86 (20.9%)	18.44 ± 13.5 (20.9%)
F	33.55	13.00 ± 8.13 (38.7%)	11.60 ± 6.78 (38.7%)
G	41.46	7.80 ± 3.94 (18.8%)	7.31 ± 3.55 (18.8%)
MEAN ± SE	55.65 ± 20	10.61 ± 4.1	10.84 ± 3.85

For the successful trials, the average dedicated time to reach the object and trigger the selection was 16.16 ± 1.17 s. As shown in Table 1, the three users who performed the experiment with two objects suffered a higher miss-rate than the rest.

3.2. FES

In order to illustrate the basic controller function, two trials of a feedback controlled joint-angle tracking divided by pauses of 2 s are exemplarily shown in Fig. 8. The upper plot shows the target angle (red) along with the actual angle (black). The lower plot outlines the required stimulation intensities.

A motion error analysis was carried out for all subjects and each trial. For analyzing the precision of reaching a selected position, at the end of each sequence the steady state error E_S between the target angle and the actually reached angle/position was calculated by

$$E_S = |r_\vartheta(k_{end}) - \vartheta(k_{end})|,$$

whereby k_{end} denotes the sampling index at the end of the trial.

For evaluation of the ability to track the angular reference, the RMS (root mean square) error was determined for each trial yielding the dynamic error

$$E_D = \sqrt{\frac{1}{k_{end} - k^* + 1} \sum_{i=k^*}^{k_{end}} (r_\vartheta(i) - \vartheta(i))^2}.$$

evaluated in a time period ranging from the sampling index k^* till the end of the trial k_{end}. In order not to include the transient effects occurring when the control system is initialized, the evaluation starts $k^* = 200$ samples (8 s) after the beginning of each trial. For both error-types, sequences with no successful BCI selection of an object were omitted from the analysis. Fig. 9 shows the exemplary results for one subject and one trial of 40 given selection tasks. The mean values for both types of error were small compared to the whole range of movement (62° for this example). Thus, selecting and reaching of at least four objects was feasible for this subject. A summary of the mean values for both error-types and the possible range of motion over all successful trials is given in Table 2. For most participants, the errors are significantly small compared to the possible movement range, yielding a good differentiation between objects.

Please cite this article as: C. Vidaurre et al., EEG-based BCI for the linear control of an upper-limb neuroprosthesis, Medical Engineering and Physics (2016), http://dx.doi.org/10.1016/j.medengphy.2016.06.010

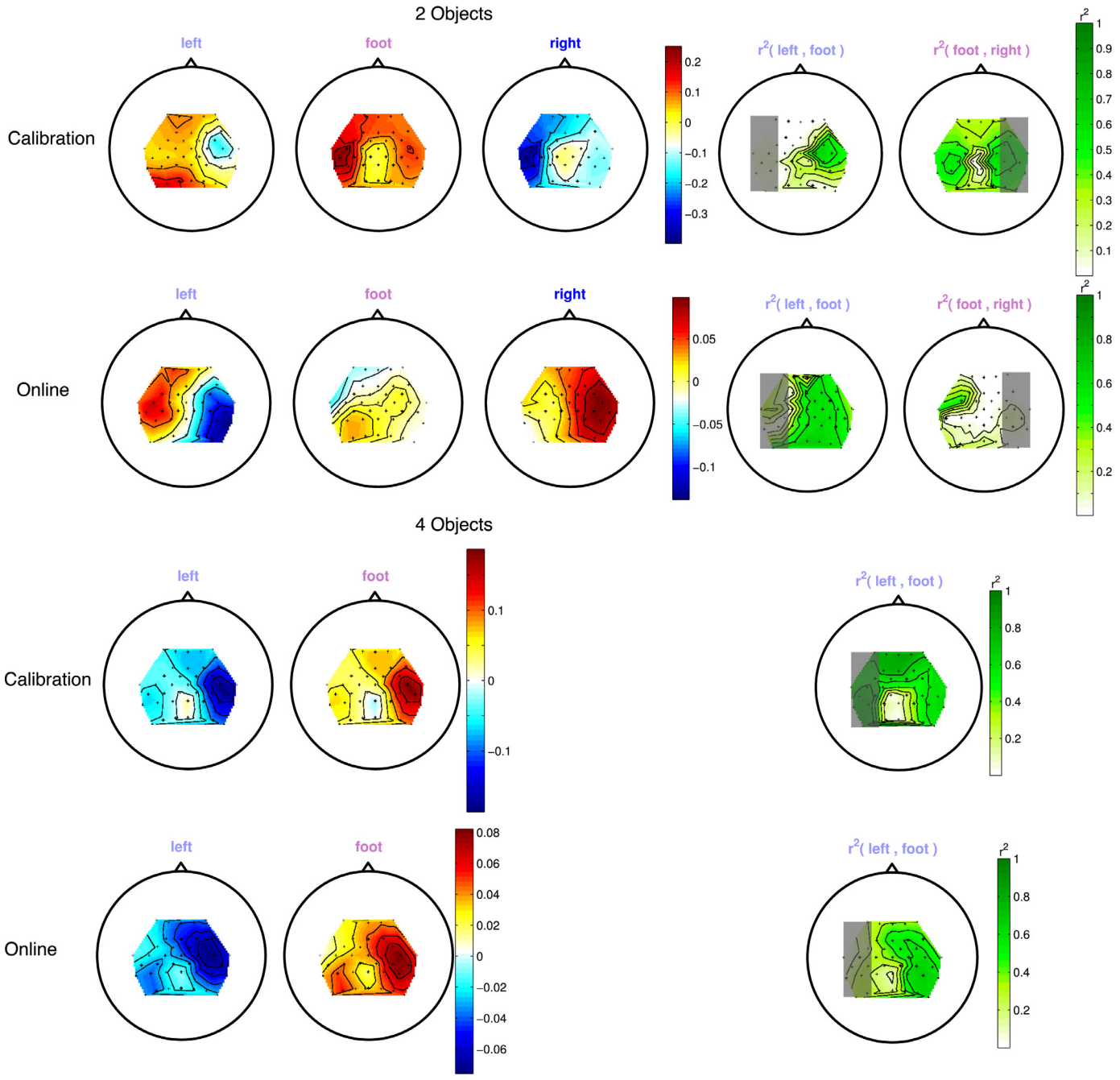

Fig. 10. Scalp maps grouped for the users who controlled the system with two objects (up, rows 1 and 2) and four objects (down, rows 3 and 4). The scalp topographies coded from blue to red (left panel) show the logarithmic power within the frequency band used during the online operation, averaged over the whole calibration recording (row 1 and 3) and online recording (rows 2 and 4). The scalp plots coded from lilac to green (right panel) display the r^2-values of the difference between the motor imagery tasks as scalp map. The shaded areas in the scalp maps of the last column correspond to the electrodes not used for the analysis and classification (see Section 2.4.3). (For interpretation of the references to colour in this figure legend, the reader is referred to the web version of this article.)

4. Discussion

The feasibility of selecting among two to four objects with linear BCI control and active FES-motion feedback control was proven for healthy subjects. The averaged percentage of successful trials was 82.50 ± 3.16%, which is comparable to the results obtained in our previous linear control study (see [13]). This accuracy is also very similar to that achieved in a previous study [31] using an ERP (event related potential) based BCI system. There, BCI participants performed the selection of objects with an average selection time of 15.38 s. This means that, even though Motor Imagery is a more challenging task than ERP, the users could control similarly well the neuro-prosthesis presented in this paper. The accuracy obtained by the participants is also significantly above the threshold for control (70% for a two-class BCI system, [30]).

The results presented in Table 2 suggest that users who performed the experiments with two objects might have slightly different brain patterns during the online operation than during the calibration. Fig. 10 shows scalp maps grouped for the users who controlled the system with two objects (up, row 1 and 2) and four objects (down, rows 3 and 4). The scalp topographies coded from blue to red (left panel) show the logarithmic power within the fre-

quency band used during the online operation, averaged over the whole calibration recording (row 1 and 3) and online recording (rows 2 and 4). The scalp plots coded from lilac to green (right panel) display the r^2-values of the difference between the motor imagery tasks as scalp map. In the case of participants who controlled two objects, one can see a bigger difference between calibration and feedback scalp plots (rows 1 and 2) than for users who controlled the system with four objects (rows 3 and 4). This effect is not translated in lower discrimination power (right panel, Fig. 10, Table 2) but might have played a role in the higher miss rate obtained by these users. A classification bias analysis showed that the system is in general not influenced by this problem. Only user B showed a more significant bias in the classification of the two classes. This was due to a lower ERD of the online left-hand trials located the right hemisphere in comparison to the calibration recording. This provoked the classifier to misclassify left-hand trials as foot trials. An analysis of the ERD/S curves showed that the discrimination differences shown in Fig. 10 were due to slightly different strength and location of the ERD/S between calibration and feedback for the users who performed the experiments with two objects. In their case, a calibration recording including some type of stimulation might improve the results. Despite this finding, those participants still obtained satisfying results.

An analysis of the possible range of motion as well as the positioning precision was performed, showing the feasibility of using a BCI–FES system for reaching objects. For five of seven tested users, the SSE and RMS are significantly smaller than the possible range of movement, demonstrating the feasibility of selecting and reaching for the majority of users. For the other two participants, it was not possible to achieve a satisfactory movement range due to a low tolerance to FES. By a simple FES-training however, this tolerance might easily be increased.

Interestingly, the users who carried out the experiments with only two selectable objects obtained also the highest Steady State errors E_s. In this case, despite the simplification of the task, the difficulty to stop the bar between thresholds was not reduced. On the contrary, the subjects who performed the experiment with four objects proved to be capable of controlling the position with a high exactitude, achieving a E_s error of 7.48 ± 0.38. For those users who suffered greater errors, the FES system might have induced the FES system might have induced muscle contractions that might have affected the position accuracy.

Another important factor in the experiment was the complexity of the task. The participants stated that the stimulation distracted them from the task when the arm did not move in the desired direction. In this respect, having selected a different limb for the neuro-prosthesis movement than for the MI tasks very likely prevented the users from being even more distracted. Although the system could then be considered less natural, the need of maintaining a high accuracy justified this decision.

4.1. Number of selectable objects

In the introduction we indicated that a good candidate to predict the accuracy of the control of the neuro-prosthesis (and therefore the number of objects that the user would be able to select) was the estimation of the accuracy from the calibration data. Subject *E* had an estimation error of 1.7 ± 3.1. However, in the post-calibration run (which served to decide whether the participant would be able to select between 2 or 4 objects), he found extremely difficult to stop the bar between the thresholds and, therefore, the experiment was performed with two objects. To explain this result, Fig. 11 depicts the r^2-values from the ERD curves between the best two classes for each subject over time computed using the online recording. When this value is high, the discriminability between classes according to the ERD is good. During the online operation, this magnitude should decrease in the moment when the user wants to select an object to be able to stop the bar between thresholds. Fig. 11 shows that the r^2-value for subject E was high, meaning good discriminability, however this participant was not able to reduce the ERD level toward the end of the trials. Consequently, the subject was not able to switch between classes (the strategy followed by most of the users to stop the bar between thresholds). This means that not only the classification accuracy, but also the latency of the ERD should be taken into account before performing experiments with such a system. Accordingly, in order to facilitate the symbol selection, when the bar was located between two thresholds, its movement was slowed down.

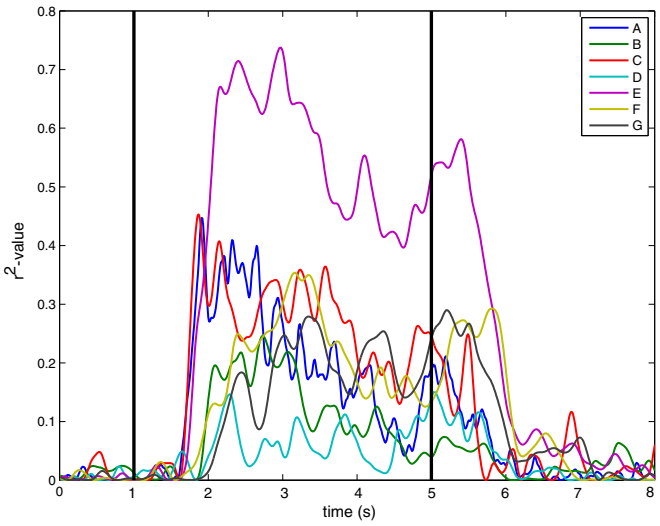

Fig. 11. r^2-values of the ERD for the best two classes of each subject averaged over trials. The two black lines denote beginning and end of trial time.

We can conclude that, in systems in which there is real-time control involved, the discriminability between classes might be an insufficient performance indicator. In our experimental design, the ability to block the movement imagination or to switch to another motor imagery class without high latency is also important. A positive correlation of the estimation of the error rate and the number of objects ($\rho = 0.7, N = 7, p = 0.08$) was found, however, this was not significant (α-level= 0.05). The correlation between the number of objects and the mean value of the r^2-value 1 s after the end of the trial was, on the contrary, significant $\rho = 0.78, N = 7, p = 0.04$ (α-level= 0.05). The statistical power was 0.7 as expected given the number of users who took part in the experiment. However, the test still shows that there is a relation between the ability to suppress the ERD and the error rate that would probably be confirmed with a higher number of users.

5. Conclusions

In this work we presented the design and implementation of a system that combines a MI-based BCI and a FES module for the linear real-time control of an upper-limb neuro-prosthesis. This study demonstrates on healthy users that it is possible to operate such a system in order to control the position of a neuro-prosthesis in a target selection task of several objects. An analysis of the possible range of motion as well as the positioning precision was performed, showing the feasibility of using this BCI–FES system for reaching objects. The results of this study constitute an accurate attempt of using a BCI to operate a FES-neuroprosthesis, setting a step toward the recovery of the control of an impaired limb with the only use of brain activity. We are aware that the system still needs to be tested in end-users. Those might suffer from higher

Please cite this article as: C. Vidaurre et al., EEG-based BCI for the linear control of an upper-limb neuroprosthesis, Medical Engineering and Physics (2016), http://dx.doi.org/10.1016/j.medengphy.2016.06.010

rates of BCI inefficiency [32,33] that might limit the application of this system (a calibration accuracy of over 80% is necessary). However, the development of new BCI training paradigms using co-adaptation has shown the potential to overcome this problem [34]. Our results show that in order to predict whether a user will be able to control the system with a higher number of objects, the ERD latency should also be taken into account. Previous work has shown that it is possible to train ERD latency, [35]. However, a simple solution would be to add a confirmation step after the selection, as has been proposed elsewhere [31]. Finally, for end-users it might be advisable to perform MI and stimulation of the same arm. Unlike for healthy participants, who repeatedly reported about the inability to perform MI simultaneously to the stimulation [24], this might not constitute a problem for end-users.

Acknowledgments

The authors thankfully acknowledge Javier Pascual for his help and dedication. They are also grateful to the reviewers for their constructive criticisms. The research leading to these results has received funding from the European Community's Seventh Framework Programme under grant MUNDUS and HUMOUR-ICT-2008-231724, the European Union's PASCAL 2 Network of Excellence (ICT-216886), the German Research Foundation DFG project KU 1453-1, DFG SPP 1527, MU 987/14-1, as well as the by the Brain Korea 21 Plus Program of the National Research Foundation of Korea funded by the Ministry of Education, Republic of Korea. This publication only reflects the authors' views. The authors declare not to have any conflicts of interest.

References

[1] Pedrocchi A, Ferrante S, Ambrosini E, Gandolla M, Casellato C, Schauer T, et al. Mundus project: multimodal neuroprosthesis for daily upper limb support. J NeuroEng Rehab 2013;10:66.
[2] Onose G, Grozea C, Anghelescu A, Daia C, Sinescu C, Ciurea A, et al. On the feasibility of using motor imagery EEG-based brain–computer interface in chronic tetraplegics for assistive robotic arm control: a clinical test and long-term post-trial follow-up. Spinal Cord 2012;50(8):599–608.
[3] Mangold S, Keller T, Curt A, Dietz V. Transcutaneous functional electrical stimulation for grasping in subjects with cervical spinal cord injury. Nature 2004;43(1):1–13.
[4] Rüdiger R, Gerner HJ. Neuroprosthetics of the upper extremity, clinical application in spinal cord injury and challenges for the future. In: Operative neuromodulation. In: Acta Neurochirurgica Supp, vol. 97/1. Vienna: Springer; 2007. p. 419–26.
[5] Ambrosini E, Ferrante S, Tibiletti M, Schauer T, Klauer C, Ferrigno G, et al. An EMG-controlled neuroprosthesis for daily upper limb support: a preliminary study. In: Conf proc IEEE Eng Med Biol Soc; 2011. p. 1–3.
[6] Müller-Putz G, Scherer R, Pfurtscheller G, Rupp R. EEG-based neuroprosthesis control: a step towards clinical practice. Neurosci Lett 2005;382:169–74.
[7] Wolpaw JR, Birbaumer N, McFarland DJ, Pfurtscheller G, Vaughan TM. Brain–computer interfaces for communication and control. Clin Neurophysiol 2002;113:767–91.
[8] Dornhege G, Millán Jd R, Hinterberger T, McFarland D, Müller K-R, editors. Toward brain–computer interfacing. Cambridge, MA: MIT Press; 2007.
[9] Muller-Putz G, Pfurtscheller G. Control of an electrical prosthesis with an SSVEP-based BCI. IEEE Trans Biomed Eng 2008;55(1):361–4.
[10] Horki P, Solis-Escalante T, Neuper C, Müller-Putz G. Combined motor imagery and SSVEP based BCI control of a 2 dof artificial upper limb. Med Biol Eng Comput 2011;49(5):567–77.
[11] Gollee H, Volosyak I, McLachlan A, Hunt K, Gräser A. An SSVEP-based brain–computer interface for the control of functional electrical stimulation. IEEE Trans Biomed Eng 2010;57(8):1847–55.
[12] Tavella M, Leeb R, Rupp R, Millán J. Towards natural non-invasive hand neuroprostheses for daily living. In: Conf proc IEEE Eng Med Biol Soc; 2010. p. 126–129.
[13] Pascual J, Velasco-Álvarez F, Müller K-R, Vidaurre C. First study towards linear control of an upper-limb neuroprosthesis with an EEG-based brain–computer interface. In: Conf Proc IEEE Eng Med Biol Soc, vol. 2012; 2012. p. 3269–73.
[14] Blankertz B, Tomioka R, Lemm S, Kawanabe M, Müller K-R. Optimizing spatial filters for robust EEG single-trial analysis. IEEE Signal Process Mag 2008;25(1):41–56.
[15] Lemm S, Blankertz B, Dickhaus T, Müller K-R. Introduction to machine learning for brain imaging. Neuroimage 2011;56:387–99.
[16] Pfurtscheller G, da Silva FL. Event-related EEG/MEG synchronization and desynchronization: basic principles. Clin Neurophysiol 1999;110(11):1842–1857.
[17] Vidaurre C, Scherer R, Cabeza R, Schlögl A, Pfurtscheller G. Study of discriminant analysis applied to motor imagery bipolar data. Med Biol Eng Comput 2007;45:61–8.
[18] Gijbels D, Lamers I, Kerkhofs L, Alders G, Knippenberg E, Feys P. The Armeo Spring as training tool to improve upper limb functionality in multiple sclerosis: a pilot study. J NeuroEng Rehab 2011;8(1):5.
[19] Shalaby R. Development of an electromyography detection system for the control of functional electrical stimulation in neurological rehabilitation. TU Berlin; 2011. [Doctoral thesis].
[20] Goodwin G, Graebe S, Salgado M. Control system design. Prentice Hall; 2001.
[21] Durfee WK, MacLean KE. Methods for estimating isometric recruitment curves of electrically stimulated muscle. IEEE Trans Biomed Eng 1989;36(7):654–667.
[22] Durfee W. Task-based methods for evaluating electrically stimulated antagonist muscle controllers. IEEE Trans Biomed Eng 1989;36(3):309–21. doi:10.1109/10.19852.
[23] Blankertz B, Tangermann M, Vidaurre C, Dickhaus T, Sannelli C, Popescu F, et al. Detecting mental states by machine learning techniques: the Berlin brain–computer interface. In: Allison B, Graimann B, Pfurtscheller G, editors. Brain–computer interfaces (revolutionizing human–computer interaction). The Frontiers Collection. Berlin, Heidelberg: Springer; 2010. p. 113–35.
[24] Vidaurre C, Pascual J, Ramos-Murguialday A, Blankertz B, Birbaumer N, Müller K-R. Neuromuscular electrical stimulation induced brain patterns improve the classification of motor imagery. Clin Neurophysiol 2013;124(9):1824–34.
[25] Kaiser V, Kreilinger A, Müller-Putz GR, Neuper C. First steps towards a motor-imagery based stroke BCI: new strategy to set up a classifier. Front Neurosci 2011;5:86.
[26] Cho W, Vidaurre C, Hoffman U, Birbaumer N, Ramos-Murguialday A. Afferent and efferent activity control in the design of brain computer interfaces for motor rehabilitation. In: Conf proc IEEE Eng Med Biol Soc; 2011. p. 7310–15.
[27] Schlögl A, Vidaurre C, Müller K-R. Brain–computer interfaces: revolutionizing human-computer interaction. Adaptive methods in BCI research—an introductory tutorial. Berlin, Heidelberg: Springer; 2010. p. 331–55.
[28] Sannelli C, Vidaurre C, Müller K-R, Blankertz B. CSP patches: an ensemble of optimized spatial filters. an evaluation study. J Neural Eng 2011;8(2):025012.
[29] Vidaurre C, Kawanabe M, von Bünau P, Blankertz B, Müller K-R. Toward unsupervised adaptation of LDA for brain–computer interfaces. IEEE Trans Biomed Eng 2011;58(3):587–97.
[30] Kübler A, Neumann N, Wilhelm B, Hinterberger T, Birbaumer N. Predictability of brain–computer communication. J Psychophysiol 2004;18(2–3):121–9.
[31] Pascual J, Lorenz R, Blankertz B, Vidaurre C. Hybrid EEG-based BCI user interface for action selection. In: Conf proc international conference on neurorehabilitation, vol. 2012; 2012. p. 763–6.
[32] Pfurtscheller G, Linortner P, Winkler R, Korisek G, Müller-Putz G. Discrimination of motor imagery-induced EEG patterns in patients with complete spinal cord injury. Comput Intell Neurosci 2009:104180.
[33] Stanton B, Williams V, Leigh P, Williams S, Blain C, Giampietro V, et al. Cortical activation during motor imagery is reduced in amyotrophic lateral sclerosis. Brain Res 2007;1172(0):145–51.
[34] Vidaurre C, Sannelli C, Müller K-R, Blankertz B. Co-adaptive calibration to improve BCI efficiency. J Neural Eng 2011;8:025009.
[35] Ramsey L, Tangermann M, Haufe S, Blankertz B. Practicing fast-decision BCI using a "goalkeeper" paradigm. BMC Neurosci 2009;10(Suppl 1):P69.

Please cite this article as: C. Vidaurre et al., EEG-based BCI for the linear control of an upper-limb neuroprosthesis, Medical Engineering and Physics (2016), http://dx.doi.org/10.1016/j.medengphy.2016.06.010